SUBMARINE PALEOSEISMOLOGY ON THE SANTA POLA FAULT (BAJO SEGURA BASIN, WESTERN MEDITERRANEAN): DERIVATING DIRECT ON-FAULT PALEOEARTHQUAKES

Paleosismología submarina en la falla de Santa Pola (Cuenca del Bajo Segura, Mediterraneo Occidental): Obteniendo el registro de paleoterremotos directamente de una falla

H. Perea (1), E. Gràcia (1), S. Martínez-Loriente (1) and R. Bartolomé (1)

(1) Barcelona-CSI, Dpt.. Geociències Marines, Institut de Ciències del Mar-CISC, Psg. Marítim de la Barceloneta, 37-49. 08003-Barcelona. hperea@icm.csic.es

Resumen/resumo: La cuenca del Bajo Segura está localizada en la terminación norte de la Zona de Cizalla de las Béticas Orientales. La evolución geológica de esta cuenca está controlada por varias estructuras activas que acomodan parte de la deformación derivada de la convergencia entre Nubia y Eurasia. La falla de Santa Pola es una de las estructuras activas localizadas en la zona marina de la cuenca. En un perfil de alta resolución hemos realizado un análisis de paleosismología submarina que ha dado como resultado la identificación de entre 6 y 10 paleoterremotos ocurridos entre 140 ka y 444 ka, resultando en un intervalo de recurrencia que varía entre 30 ka y 50 ka. También ha sido posible obtener una tasa de deslizamiento vertical, el salto vertical por evento y la magnitud máxima para cada uno de ellos.

Palabras clave: Paleosismología submarina, Fallas activas, Sísmica de alta resolución, Cuenca del Bajo Segura.

***Abstract**: The Bajo Segura basin is located at the northern termination of the East Betic Shear Zone. The geological evolution of this basin is controlled by a number of active faults and folds that accommodates part of the deformation driven by the convergence between the Nubian and Eurasian plates. The Santa Pola fault is one of the active structures located on the offshore of the Bajo Segura basin. In a high resolution sparker single channel seismic profile we have performed a submarine direct on-fault paleoseismic analysis resulting in the identification of 5 to 10 post-seismic growth sequences. These sequences may be related to 6 to 10 paleoearthquakes occurred between 140 ka and 444 ka, accounting for a recurrence interval ranging from 30 ka to 50 ka. It has also been possible to obtain a long term vertical slip rate, the vertical slip per event and the maximum magnitude of each one.*

***Key words**: Submarine paleoseismology, Active faults, High resolution seismics, Bajo Segura Basin.*

INTRODUCTION

The East Betic Shear Zone (EBSZ) is a large left-lateral strike-slip fault system of sigmoid geometry (figure 1) (Silva *et al.*, 1993) that accommodates part of the deformation driven mainly by the NW-SE convergence (4-5 mm/yr) between the Nubian and Eurasian plates (Nocquet, 2012). The Bajo Segura fault zone (BSFZ) is the northern terminal splay of the EBSZ (figures 1 and 2).

This area is marked by moderate to low instrumental seismic activity and magnitude earthquakes (figures 1). Nevertheless, this zone has been affected by moderate to large historical earthquakes of which the largest is the 1829 Torrevieja earthquake (IEMS98 IX-X) (Martínez Solares and Mezcua, 2002). The BSFZ comprises active faults and folds resulting from the transpressive setting established since the Plio-Pleistocene (i.e. Alfaro *et al.*, 2012; Perea *et al.*, 2012).

Here we focus on the Santa Pola Fault (SPF3 in figure 2) an offshore fault of the BSFZ, and present the results of the direct on-fault submarine paleoseismological study carried out in this fault using the high-resolution sparker single channel seismic (SCS) profiles acquired during the marine geophysical EVENT-SHELF cruise (2008).

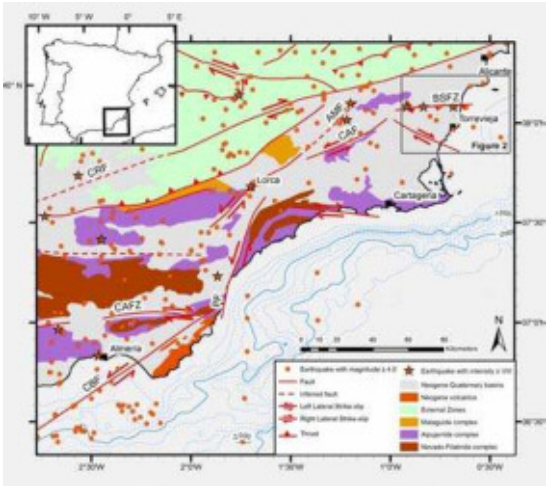

Figura 1: Mapa geológico del sureste de la Península Ibérica (Sanz de Galdeano *et al.*, 1995). Terremotos (IGN, 2013); estrellas rojas: históricos; puntos rojos: instrumentales. AMF: Falla de Alhama de Murcia; BSFZ: Zona de falla del Bajo Segura; CAF: Falla de Carrascoy; CAFZ: Zona de falla del Corredor de la Alpujarras; CBF: Falla de Carboneras; CRF: Falla de Crevillente; PF: Falla de Palomares. Inserción: Mapa de la Península Ibérica.
Figure 1. Regional geological map (*Sanz de Galdeano et al.*, 1995) *of the southeastern Iberian margin. Earthquakes (IGN, 2001); red stars: historical; red dots: instrumental. AMB: Alhama de Murcia fault; BSFZ: Bajo Segura fault zone; CAF: Carrascoy fault; CAFZ: Corredor de la Alpujarras fault zone; CBF: Carboneras fault; CRF: Crevillente fault; PF: Palomares fault. Inset: Iberian Peninsula map.*

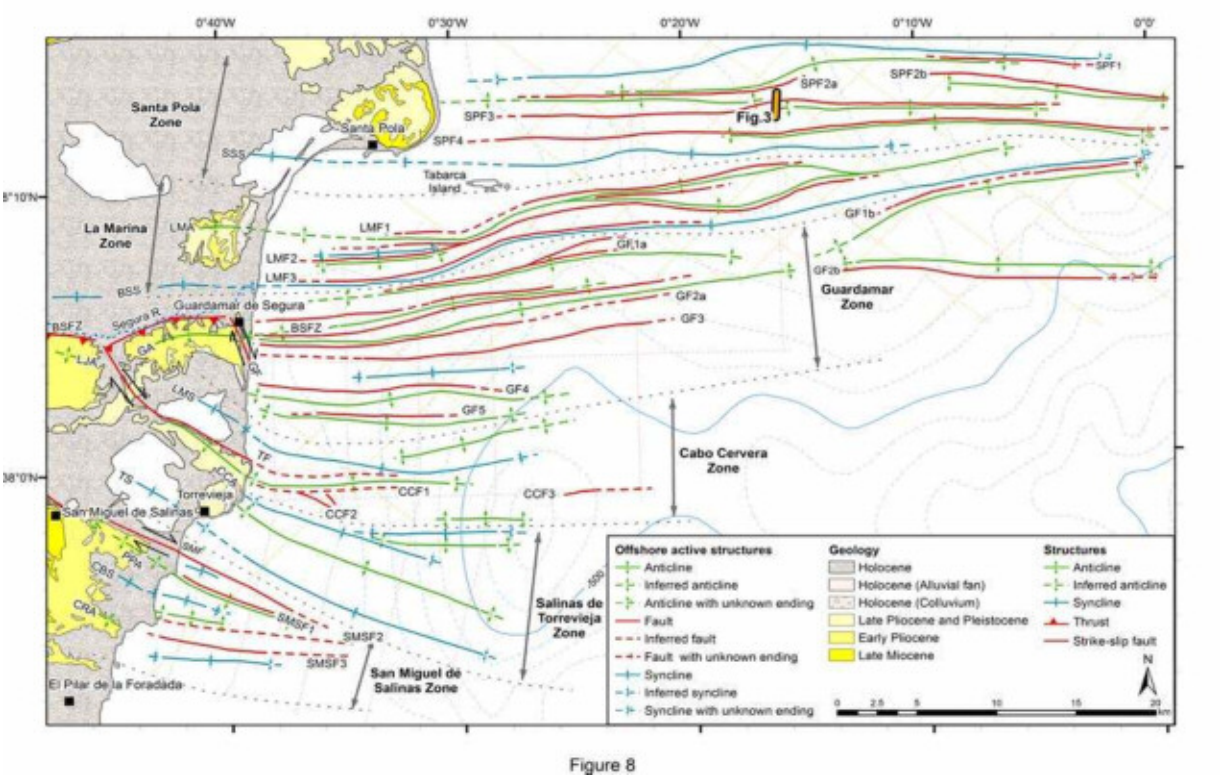

Figure 8

Figura 2. Mapa geológico (Alfaro *et al.*, 2002) y batimétrico de la cuenca del Bajo Segura mostrando las estructuras geológicas activas situadas en el mar (Perea *et al.*, 2012). Fallas: BSFZ: Zona de falla del Bajo Segura; GF: Falla de Guardamar; SMF: Falla de San Miguel de Salinas; TF: Falla de Torrevieja. Pliegues: BSS: Sinclinal del Bajo Segura; CBS: Sinclinal de Cala del Bosque; CCA: Anticlinal de Cabo Cervera; CRA: Anticlinal de Cabo Roig; GA: Anticlinal de Guardamar; LJA: Anticlinal de Lomas de la Juliana; LMA: Anticlinal de La Marina; LMS: Sinclinal de La Mata; PPA: Anticlinal de Punta Prima; SSS: Sinclinal de Salinas de Santa Pola; TS: Sinclinal de Torrevieja.

Figure 2. Geological (Alfaro *et al.*, 2002) *and bathymetric map of the Bajo Segura basin showing the offshore active geological structures* (Perea *et al.*, 2012). *Faults: BSFZ: Bajo Segura fault zone; GF: Guardamar fault; SMF: San Miguel de Salinas fault; TF: Torrevieja fault. Folds: BSS: Bajo Segura syncline; CBS: Cala del Bosque syncline; CCA: Cabo Cervera anticline; CRA: Cabo Roig anticline; GA: Guardamar anticline; LJA: Lomas de la Juliana anticline; LMA: La Marina anticline; LMS: La Mata syncline; PPA: Punta Prima anticline; SSS: Salinas de Santa Pola syncline; TS: Torrevieja syncline.*

THE BAJO SEGURA BASIN

The Bajo Segura basin is located in the Eastern Betic Cordillera (SE Spain) and extends eastwards into the Mediterranean Sea (figures 1 and 2). The basin is infilled by a succession of Upper Miocene to Quaternary sedimentary units (Montenat, 1977; Alfaro *et al.*, 2012). This sedimentary cover overlies a basement forming part of the Internal Zone of the Betic Cordillera (Triassic calcareous metamorphic rocks of the Alpujarride complex).

A transpressive regime is influencing the geologic evolution of the Bajo Segura basin area, with a NNW-SSE compressive stress field from the upper Miocene to the Present (Silva *et al.*, 1993; Alfaro *et al.*, 2012). It has been reported a number of faults and folds affecting the Plio-Quaternary sedimentary units (i.e. Alfaro *et al.*, 2012; Perea *et al.*, 2012) providing evidence of recent Quaternary activity in the Bajo Segura basin (figure 2).

Perea et al. (2012) identified up to six units (I1 to I6) on the high-resolution sparker SCS profiles that are bounded by five horizons (H1 to H5). These authors relate the horizons to regional erosional surfaces produced during the Quaternary global sea level lowstands and, thus, they could be correlated with Marine Isotopic Stages (MIS): a) H1 to MIS2 (20 ka); b) H2 to MIS6 (135 ka); c) H3 to MIS8.2 (247.6 ka); d) H4 to MIS10 (341 ka); and e) H5 to MIS 12 (434 ka).

SUBMARINE PALEOSEISMOLOGY: SANTA POLA FAULT

Submarine paleoseismology merge and integrate two well-established disciplines, paleoseismology and marine geology, to detect and describe the occurrence of paleoearthquakes on faults located underwater. Recently, the identification of active fault growth sequences on high-resolution seismic profiles has allowed to derive the submarine paleoearthquake records directly on-fault (i.e. coseismic vertical increments of displacement) (Brothers *et al.*, 2009; Barnes and Pondard, 2010).

The Santa Pola fault (SPF3 in figures 2 and 3) strikes approximately E-W and has a length of about 35 km. The high-resolution sparker SCS profile EVS-29 (figure 3) images a vertical fault that is folding and offsetting horizons H5 and H3, and probably would have affected horizon H2 but this is eroded across de

fault zone. Below unit I3 seems that sedimentation has been continuous, although horizon H4 have not been identified in the area. Moreover, in the profile EVS-29 it could be observed that units at each side of the fault zone do not present the same thickness. All these observations points to that fault as a valid case to perform a direct on-fault paleoseismological study (Barnes and Pondard, 2010).

To perform the paleoseismological analysis the same reflectors have been identified on the downthrown and upthrown blocks and the accumulated vertical displacement for each reflector has been calculated.

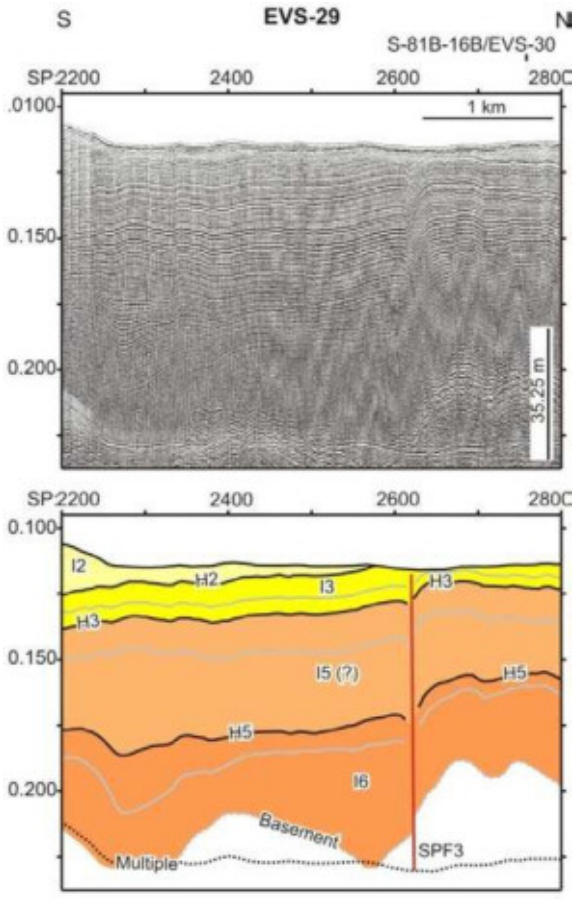

Figura 3: Detalle del perfil de alta resolución SCS de sparker EVS-29 en la zona de Santa Pola (ver localización en la figura 2) y la interpretación que muestra las unidades sismo-estratigráficas y la falla de Santa Pola (SPF3) (Perea et al., 2012).

Figure 3. Detail of the high-resolution sparker SCS profile EVS-29 in the Santa Pola zone (see location in figure 2) and line drawing showing the seismo-stratigraphic units and Santa Pola fault (SPF3) (Perea *et al*., 2012).

To this calculation it has been assumed a sound veolocity of 1600 m/s. Figure 4 shows the plot of the vertical displacement accumulation through time estimated on profile EVS-29.

DISCUSSION AND CONCLUSIONS

From the analysis of figure 4 we calculate a vertical accumulated displacement of 7.1 m in 257 ka (from 184 ka to 441 ka). This allow us to estimate a vertical slip rate for the Santa Pola fault of about 0.03 mm/a. We should consider the possibility that this could be a strike-slip fault with vertical movement and, thus, this slip rate should be considered as minimum.

Regarding the interpretation of the obtained plot two possible scenarios are discussed depending on the number of post-seismic growth sequences recognized. These sequences are identified on the basis of a change from a section of the curve approximately flat to an inclined one (Barnes and Pondard, 2010). The first one corresponds to the identification of 5 post-seismic growth sequences, implying the occurrence of 6 paleoeathquakes in a period of about 300ka (between 140 ka and 444 ka). This gives a recurrence of 50 ka between events. However, it could be discussed the existence of a cluster of seismicity between 408 ka and 444ka. In this case there are 4 events in 36ka, one event every 9 ka, and after two events in 264 ka. The calculated vertical displacement for each event ranges between 0.1 m to 1.6 m to obtain magnitudes between 6.0 and 7.1 using the relationships from Wells and Coppersmith (1994).
The second scenario points to the occurrence of 10 paleoearthquakes related to the observation of 10 post-seismic growth sequences. These events may have occurred also during 300 ka resulting in a recurrence of 30 ka. Nevertheless, two clusters of events could be discussed. The first one is composed by 5 events during 48 ka (from 396 ka to 444 ka), which gives a recurrence around 9.6 ka. The second cluster could include 3 events during 36 ka (between 309 ka and 345 ka) giving a recurrence of 12 ka. The last 2 events, to sum the 10 paleoearthquakes, may have occurred between 198 ka and younger than 143 ka. The vertical displacement for each event is between 0.1 m to 1.3 m. The magnitudes corresponding to these displacements range from 5.9 to 7.0 according to the Wells and Coppersmith (1994) relationships.

To conclude, it has been calculated a vertical slip rate of 0.03 mm/a for the Santa Pola fault. Furthermore, this fault is capable to produce large earthquakes. We have identified between 5 and 10 post-seismic growth sequences that imply the occurrence of 6 to 10 paleoearthquakes between 140 ka and 444 ka, accounting for a recurrence interval between 30 ka and 50 ka. The vertical displacement for each event ranges from 0.1 m to 1.6m and the estimated magnitude may vary between 5.9 and 7.1. Nevertheless, all this data has a large uncertainty since the age of the reflectors is based on the correlation of the horizons H1 to H5 with Marine Isotopic Stages. To improve our knowledge about the age of these horizons some coring and dating should be necessary.

Agradecimientos: The authors acknowledge the support of the Spanish Ministry of Science and Innovation through National Projects IMPULS (REN2003-05996MAR), EVENT (CGL 2006-12861-C02-02) and SHAKE (CGL 2011-30005-C02-02); Acciones Complementarias EVENT-SHELF (CTM 2008-03346-E/MAR) and SPARKER (CTM 2008-03208-E/MAR); and ESF TopoEurope TOPOMED project (CGL 2008-03474-E/BTE). Hector Perea is fellow researcher at ICM-CSIC under the Juan de la Cierva contract nº JCI-2010-07502 funded by the Spanish Ministry of Science and Innovation.

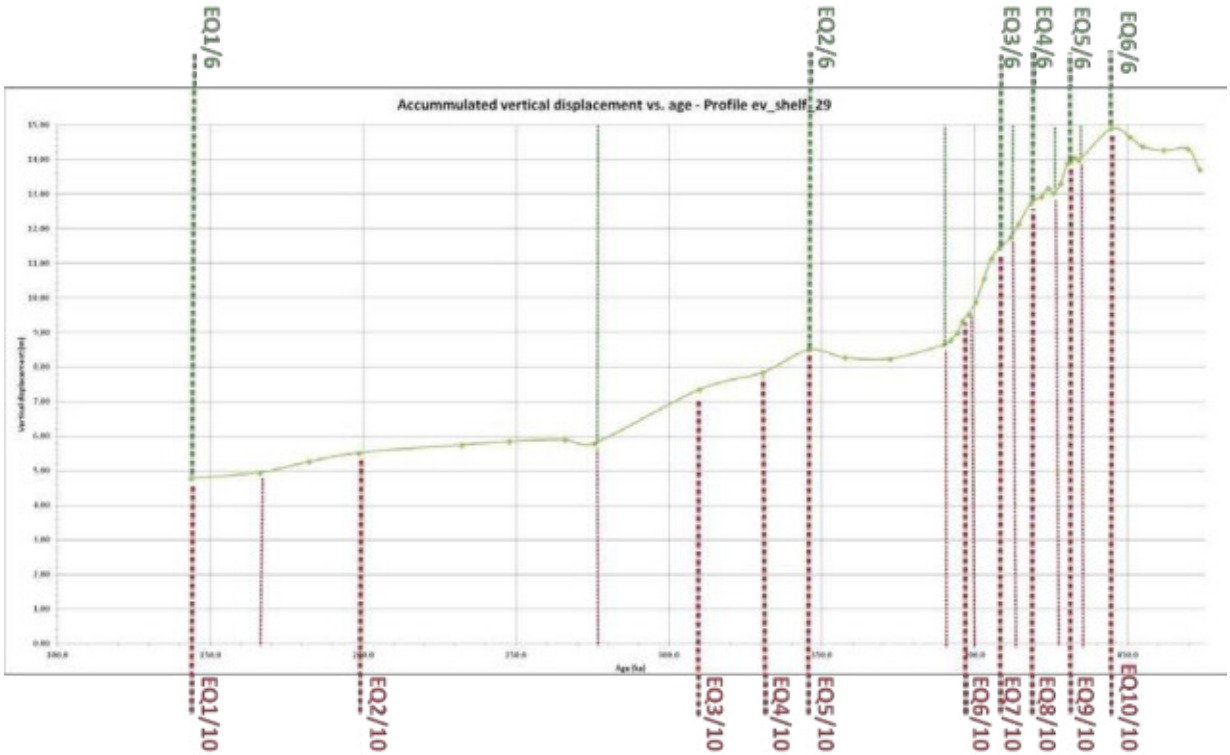

Figura 4: Gráfica que muestra el desplazamiento acumulado con el tiempo, derivado de las diferentes elevaciones estructurales medidas en cada bloque de la falla de Santa Pola en el perfil EVS-29. Se muestran dos interpretacfiones diferentes de paleoterremotos, una mas conservativa (10 eventos; en rojo) y una menos (6 eventos; en verde).

Figure 4. Plot of vertical displacement accumulation through time, derived from structural elevation differences measured across each end of the profile EVS-29. Two different interpretation of paleoearthquakes are shown, the most (10 events; red) and the less (6 events; green) conservatives.

References

Alfaro, P., Andreu, J.M., Estévez, A., Soria, J.M. & Teixidó, T. (2002). Quaternary deformation of the Bajo Segura blind fault (eastern Betic Cordillera, Spain) revealed by high-resolution reflection profiling: *Geological Magazine*, 139, 331–341.

Alfaro, P., Bartolome, R., Borque, M.J., Estévez, A., García-Mayordomo, J., García-Tortosa, F.J., Gil, A.J., Gràcia, E., Lo Iacono, C. & Perea, H. (2012). The Bajo Segura Fault Zone: Active blind thrusting in the Eastern Betic Cordillera (SE Spain): *Journal of Iberian Geology*, 38, 271–284.

Barnes, P.M. & Pondard, N. (2010). Derivation of direct on-fault submarine paleoearthquake records from high-resolution seismic reflection profiles: Wairau Fault, New Zealand: *Geochemistry Geophysics Geosystems*, 11.

Brothers, D.S., Driscoll, N.W., Kent, G.M., Harding, A.J., Babcock, J.M. & Baskin, R.L. (2009). Tectonic evolution of the Salton Sea inferred from seismic reflection data: *Nature Geoscience*, 2, 581–584.

IGN (2013). *Catálogo de terremotos en el área de la Península Ibérica e Islas Canarias* (http://www.ign.es/ign/layoutIn/sismoFormularioCatalogo.do). Last access October 2013.

Martínez Solares, J.M. and Mezcua, J. (2002). *Catálogo sísmico de la Península Ibérica (880 a.C.-1900) (Monografía núm.18)*: Dirección General IGN.

Montenat, C. (1977). *Les bassins néogènes et quaternaires du levant d'Alicante à Murcie (Cordilères Bètiques Orientales, Espagne), Stratigraphie, paléontologie et évolution dynamique*. Phd Thesis. University of Lyon.

Nocquet, J. (2012). Present-day kinematics of the Mediterranean: A comprehensive overview of GPS results: *Tectonophysics*, 579, 220-242.

Perea, H., Gràcia, E., Alfaro, P., Bartolomé, R., Lo Iacono, C., Moreno, X., Masana, E. & Team, E.-S. (2012). Quaternary active tectonic structures in the offshore Bajo Segura basin (SE Iberian Peninsula – Mediterranean Sea): *Nat. Hazards Earth Syst. Sci.*, 12, 3151–3168.

Sanz de Galdeano, C., López, C., Delgado, J. & Peinado, M.A. (1995). Shallow seismicity and active faults in the Betic Cordillera. A preliminary approach to seismic sources associated with specific faults: *Tectonophysics*, 248, 293–302.

Silva, P.G., Goy, J.L., Somoza, L., Zazo, C. & Bardají, T. (1993). Landscape response to strike-slip faulting linked to collisional settings: Quaternary tectonics and basin formation in the Eastern Betics, southeast Spain: *Tectonophysics*, 224, 289–303.

Wells, D.L. & Coppersmith, K.J. (1994). New empirical relationships among magnitude, rupture length, rupture area and surface displacement: *Bull.Seismol.Soc.A.*, 84, 974–1002.